Characterization of Functional States in Nicotine- and Cotinine-Imprinted Poly(4-vinylphenol) Films by Nanoindentation

Asta Richter,[1] Joseph J. BelBruno[2]

[1]*Department of Engineering, Technical University of Applied Sciences Wildau, 15745 Wildau, Germany*
[2]*Department of Chemistry, Dartmouth College, Hanover, New Hampshire 03755*

Received 12 April 2011; accepted 17 July 2011
DOI 10.1002/app.35270
Published online 3 November 2011 in Wiley Online Library (wileyonlinelibrary.com).

ABSTRACT: Thin, imprinted poly(4-vinylphenol) (PVP) films were produced by spin coating using nicotine or its metabolite, cotinine, as template molecules. The template molecules were extracted from these films and later reloaded (or cross-loaded) from solution. Depth sensing nanoindentation was applied to measure the nanomechanical properties of the imprinted polymer films. Changes in the nanomechanical properties were correlated to the functional state of the imprinted polymer, allowing identification of the films in their "as produced" state, "template removed state or "reloaded" state. In addition, the nanomechanical properties were capable of identifying which of the two template molecules were inserted in to a film. Reinsertion of a template molecule into a "template removed" film was found to increase the nanohardness over the values recorded for the "as produced" film. This behavior was discussed in terms of the hydrogen bonding characteristics of the materials (through density functional calculations) and the physical properties of poly(4-vinylphenol) coatings. © 2011 Wiley Periodicals, Inc. J Appl Polym Sci 124: 2798–2806, 2012

Key words: molecularly imprinted polymer; nanoindentation; nanohardness; density functional theory (DFT) calculations

INTRODUCTION

Molecular imprinting is a technique that allows for the production of molecule specific receptors that are analogous to biological receptor binding sites without the cost or environmental sensitivity of the natural systems.[1–5] Molecularly imprinted polymers (MIPs) may be based on either covalent or noncovalent binding between the host polymer and the target or template molecule. The wet phase inversion procedure[6–9] for preparation of MIPs involves a polymerized starting material that is dissolved with the template in a theta solvent. A template-host network is allowed to form in solution and precipitated by immersion in a nonsolvent. Originally developed to produce MIP membranes, we have adapted this procedure to the production of thin, 300 nm to 5 μm, films via spin coating[10–12] and hydrogen bond interactions between the template and host polymer.

Nicotine is a characteristic component of tobacco smoke, and cotinine is a major metabolite of nicotine that is detected in the urine of smokers. Other reports of nicotine MIPs have appeared in the literature. For example, a nicotine-targeted MIP based on the synthesis of the polymer from methacrylic acid monomers has been previously reported.[13] In this report, we describe the production of a poly(4-vinylphenol) (PVP)-based MIP film produced by combining the phase inversion process with spin coating. We have previously reported[14,15] on the use of depth sensing nanoindentation[16–23] to study the nanomechanical properties of MIP films. We have reported the nanohardness and elastic modulus to be dependent upon the functional state of the MIP. That is, whether the MIP is in an "as-produced" state, has had the template molecule removed or has had the template (or a related molecule) reinserted into the emptied MIP. In this report, we describe these nanomechanical measurements for the nicotine- and cotinine-containing MIPs and provide a rationale for the observed changes in these measurements with changing functional state.

EXPERIMENTAL

Production of MIP films

Poly(4-vinylphenol) is a less commonly used polymer, but its aromatic nature and hydrogen bonding potential make PVP an ideal host matrix for MIPs.

Additional Supporting Information may be found in the online version of this article.

Correspondence to: J. J. BelBruno (jjbchem@dartmouth.edu).

Contract grant sponsor: Harris German-Dartmouth Distinguished Visiting Professorship (Dartmouth College).

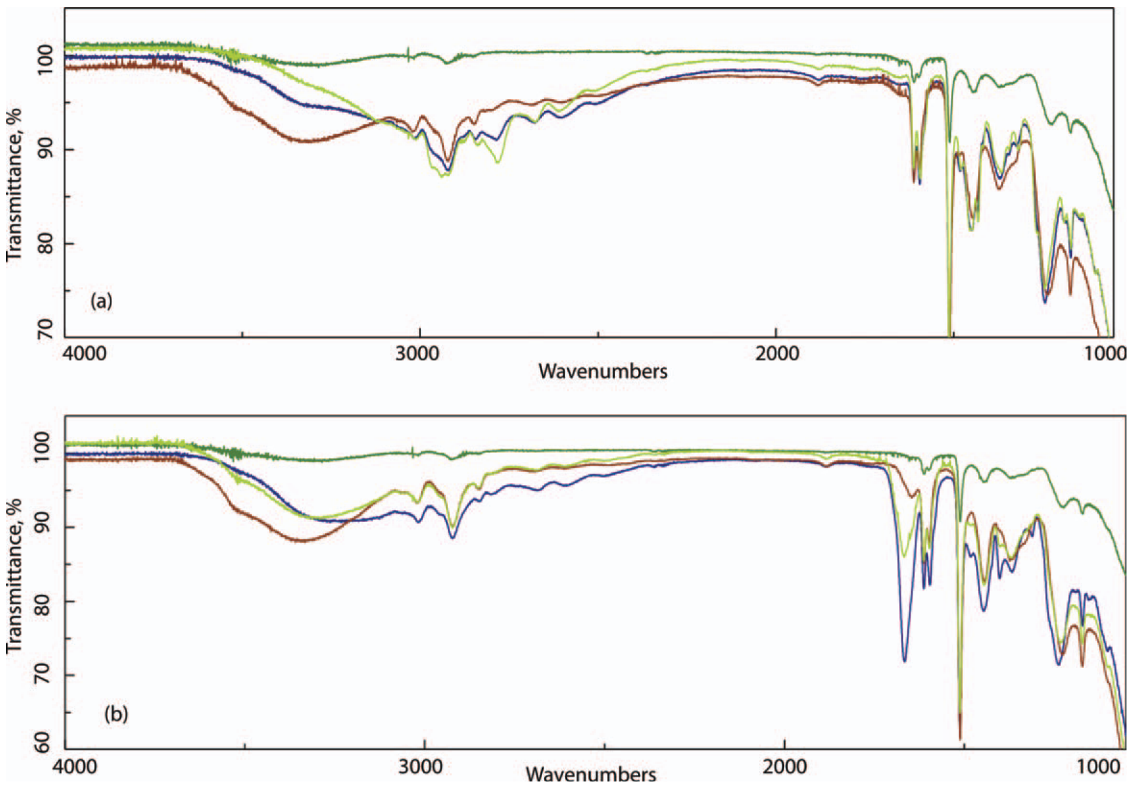

Figure 1 Control (dark green), as produced MIP (blue), template extracted MIP (red) and template reinserted MIP (light green) infrared spectra for (a) nicotine and (b) cotinine templated films. [Color figure can be viewed in the online issue, which is available at wileyonlinelibrary.com.]

The PVP films are produced by spin coating; a simple deposition technique that is sensitive to the composition and viscosity of the solution and the rotating speed of the plate.[24]

Solutions composed of 10 mL of methanol (Acros Organics; ACS Reagent Grade 99.8%) with 10 wt % of PVP powder obtained from Polysciences, Inc. (MW = 22,000; T_g 150°C) and 5 wt % of nicotine (Sigma-Aldrich; PESTANAL® Analytical Standard) or cotinine (Sigma; ~ 98%) were nitrogen purged, covered, and stirred at room temperature for 24 h. Control films (NIPs) were similarly produced but without the nicotine or cotinine. This procedure differs from the conventional MIP production process and is related to the so-called phase inversion production method. It is a preferred process for film production, as MIPs produced by the conventional process would still require later dissolution before casting. Films were spin cast from these solutions onto 22-mm-square glass microscope cover slips. Typically, the slides are cleaned in nitric acid and then prewashed on the spin coater with spectroscopic grade isopropanol and acetone before polymer deposition. The coating solution was dropped onto a stationary substrate, and the spin coater was operated at 4000 rpm for 30 s with negligible ramp up time. The rotation spreads the solution evenly over the surface and also causes the solvent to evaporate leaving a thin film of solid material on the substrate. The concentration of PVP in the casting solution is the dominant variable for the film thickness, which increases rapidly with increasing concentration (solution viscosity), as shown in previous reports.[10] We have not completed a comprehensive study of film thickness as a function of these parameters but have measured the thickness of films made under the conditions cited here to be typically near 1 μm. Cast films are quite stable and may be stored for an indefinite time.

The template molecule was removed from the film by immersion in deionized water for 5 h. Nicotine (or cotinine) removal was confirmed by FTIR measurements. Template reinsertion (or reinsertion of the complementary template molecule) was accomplished by immersion of the template extracted (or control) film in a 5 wt % solution of the template molecule in deionized water for 2.5 h. This reinsertion, as with the template removal procedure, is an equilibrium-controlled process and reinsertion occurs to ~ 50% of the initial concentration (via qualitative FTIR measurements). Additional immersion time was not found to increase the relative amount of template molecule reinserted into the film. FTIR spectra were recorded at 1 cm^{-1} resolution over the energy range from 4000 to 1000 cm^{-1}. Typical spectra are shown in Figure 1 for both templates. In terms of qualitative indications of template presence, the band between ~ 3400 and 2900 cm^{-1} for the —OH stretch of PVP broadens, and some of the weak discrete transitions grow in when hydrogen bonded to nicotine or cotinine. In addition, at ~ 1700 cm^{-1}, the presence of the carbonyl band of cotinine confirms the interaction of that template with the polymer in the film. The presence of either template will result in the observation of a weak carbon–carbon band at ~ 1500 cm^{-1}. The surface topography of the films is characterized by average roughness measurements, R_a, using scanning force microscopy (SFM). It is defined as the average deviation of the profile from a mean line or the average distance from the profile to the mean line over the length of the assessment. The surface roughness, R_a, is given by the sum of the absolute values of all the areas above and below the mean line divided by the sampling length.

Nanoindentation measurements

All nanoindentation experiments were performed using the electrostatic transducer of the Hysitron triboscope in the UBI 1 as described in a previous publication.[25] Briefly, the data consist of a load-displacement curve. For soft samples such as polymers, the stiffness of the internal springs holding the indenter must be subtracted from the applied load to obtain the sample stiffness. Hardness, H, is calculated in the now standard format,[17] as the applied load, F, divided by the area, A_c, of the indenter tip at the contact depth, h_c; the area is depth dependent. The modulus is derived from the slope of the load-displacement curve upon unloading when the sample elastically recovers. Investigations are performed with a blunted 90° diamond cube corner tip. The calibration of the tip to determine the depth dependent area function $A_c(h_c)$ was obtained with the standard curve-fitting method using fused quartz with its known reduced modulus as the reference material. Additionally, calibration with a sharp silicon grating was performed.[26] Thermal drift is measured and the effect is compensated in the resulting data. Typical drift rates range up to 0.5 nm/s. The penetration depth of the indent should not exceed 30% of the polymer film thickness to avoid substrate effects. Our experiments have been performed with penetration depths less than 30% of the total thickness.

If loading and unloading are repeatedly performed at the same location on the sample surface, depth dependent mechanical properties are obtained.[15,18,21] Eight cycles of multi-indentation have been performed to calculate the depth dependent hardness and the indentation modulus, as shown in Figure 2. As described in previous reports,[25] multicycling means, after loading to a maximum load,

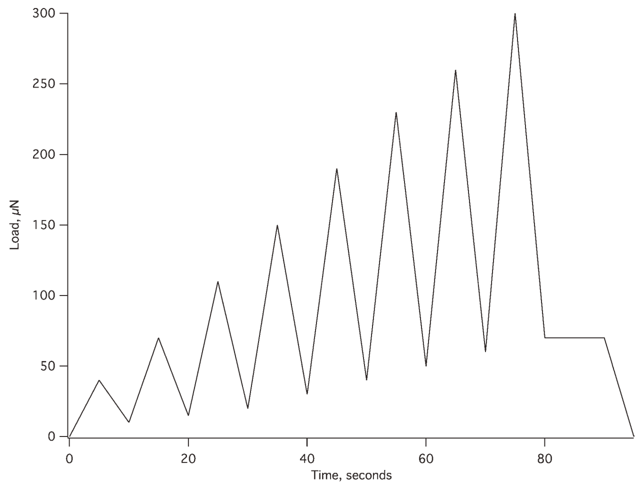

Figure 2 Load-time function for multi-indents with eight cycles as used in this study.

F_{max}, the sample is partially unloaded to a minimum load, $F_{min} = 0.1$ to $0.25\ F_{max}$, required to prevent the tip from losing contact with the sample and sliding to a new lateral position. The sample is then reloaded to the same or an increased maximum load ($F_{max} + \Delta F$) and the cycle is repeated. Multicycling delivers a set of data that includes the entire material response. Average values are obtained from several measurements at different locations on the same sample set.

COMPUTATIONAL DETAILS

All optimizations were performed with NWChem, a Computational Chemistry Package for Parallel Computers, v5.1,[27] with no symmetry or geometric constraints. The correlation and exchange effects were calculated using the Perdew-Burke-Ernzerhof (PBE) exchange-correlation functional[28] with the 6-31G* basis set[29] for all atoms. Several initial orientations of the PVP molecule(s) relative to nicotine or cotinine were optimized to ensure that the total energy of the complex was not dependent upon this factor. All calculations were run in parallel on a Linux cluster comprised of 94 Quad-Core (2x) AMD Opteron nodes (752 cpus) and 6 Quad-Core (2x) Intel nodes (48 cpus). In aggregate, the Linux cluster has 3 terabytes of memory and more than 35 terabytes of disk space. Geometric structures were visualized using Avogadro.[30]

RESULTS AND DISCUSSION

Control PVP and MIP film general features

The structure of the MIP and NIP films depends upon several factors. These include temperature and spin casting conditions such as speed and deposition

TABLE I
Measured Surface Roughness Over a 130 × 130 μm Nicotine Film Sample

Functional state[a]	R_a (nm)
NIP	11.5
As produced	69.2
Template removed	44.1
Template reinserted	33.1

[a] Functional state definition: PVP-X indicates an "as produced" MIP where N = nicotine and C = cotinine); PVP-X-Y indicates a MIP imprinted with X, which is subsequently removed and Y is inserted from solution.

time, and the PVP concentration of the solution. Measured values for surface roughness, R_a, for a 130 μm square measurement area of nicotine films are presented in Table I. The pure PVP films deposited from the casting solution containing 10% polymer have a characteristically smooth morphology. In the investigations presented in this article, the pure PVP NIP film has a surface roughness of 11.5 nm. No significant morphological features are found in the control PVP films; i.e., the films are flat. The "as produced" MIP films containing nicotine template molecules show a different surface morphology in comparison to the control films. Surface stripes, representing different heights, are the main surface feature. The surface roughness of this type of sample was measured to be 69.2 nm. SFM images on the stripes as shown in Figure 3(a) represent flat areas with a nanosize ripple structure. Removal of the nicotine from the MIP results in a loss of the stripe morphology and the observation of a number of pores in the surface, Figure 3(b). The pores are apparently formed during the solidification process of the polymer films and are caused by the presence of the template molecules and the porogen solvent during the film growth process.[12] The assumption is that the pores are present in the "as produced" samples but lie beneath the stripe morphology. The template molecules are smaller than the size of the pores observed in our films. The additional volume of the measured pores results in part from the geometrical form of the template molecule, the arrangement of that molecule within the polymer host, and the evaporation of the solvent through the solidifying polymer film. Pores are a desirable property for the MIPs; they allow for more contact between an analyte solution and molecular cavities within the bulk of the film. The surface roughness of the nicotine-removed MIP is 44.1 nm. Reinsertion of nicotine into this MIP partially restores the strip morphology but has minimal effect on the roughness of the surface (R_a = 33.1). The different film morphology in the SFM images is characteristic for the presence or absence of the template molecules.

Nanomechanical properties

The elastic behavior of pure PVP films occurs by deformation of the polymer molecules and movement of the chains after the adhesion energy has been overcome. Contact pressure (hardness) will vary even for homogeneous matter such as the control sample, as the deformation starts with purely elastic deformation, and after yielding, the plastic contributions increase. Multicycling also allows to study visco-elasto-plastic properties of the polymer.[15]

Typical multicycling load-displacement curves for MIP films with nicotine and cotinine template molecules in the casting solution for the spin coating process are shown in Figure 4. From the load-displacement curves in Figure 4(a), it is clear that the "as produced" nicotine-loaded MIP films, PVP-N for

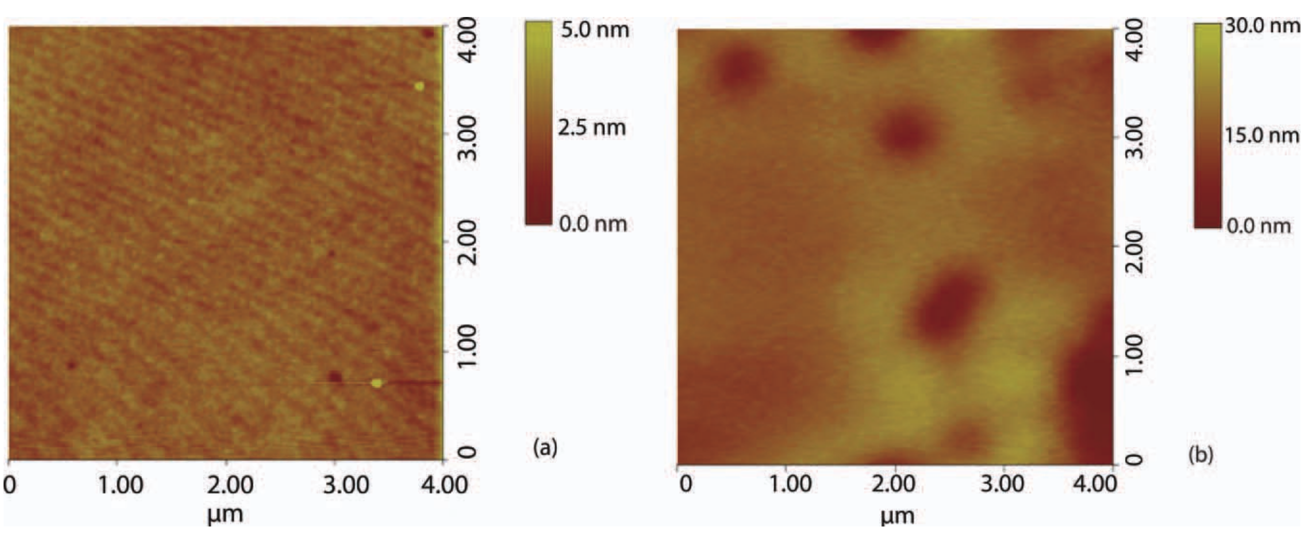

Figure 3 SFM images of size 4 × 4 μm of (a) an "as produced" nicotine imprinted film and (b) a "nicotine removed" imprinted film. [Color figure can be viewed in the online issue, which is available at wileyonlinelibrary.com.]

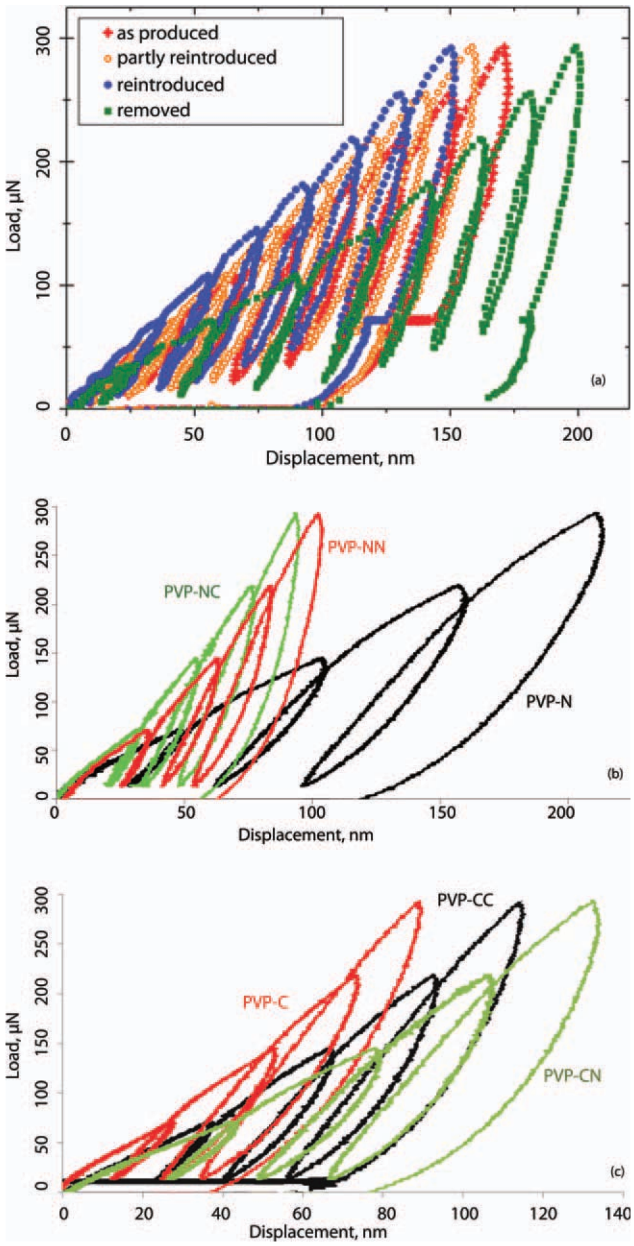

Figure 4 Load-displacement curves (a) as average values for nicotine imprinted PVP samples and specific examples of reloading with the original or alternative template in (b) nicotine-based PVP-N and (c) cotinine-based PVP-C. PVP-X indicates an as produced MIP: N = nicotine and C = cotinine); PVP-X-Y indicates a MIP imprinted with X, which is subsequently removed and Y is inserted from solution. [Color figure can be viewed in the online issue, which is available at wileyonlinelibrary.com.]

example, have average indentation depths of ~ 175 nm with a maximum applied load of 300 μN; removal of the nicotine increases the penetration depth to nearly 200 nm. Surprisingly, reinsertion of nicotine reduces the penetration depth to a value 35 nm less than that of the original imprinted film. Clearly, the reintroduced presence of the template molecule in the MIP leads to a stiffer film. Analogous results are obtained for the cotinine-imprinted films. The assignment of the basis of the change in nanomechanical properties to the template is reinforced by the fact that a MIP with the template removed is less stiff than a pure PVP film for the same applied load. The process of reloading nicotine-based PVP-N and cotinine-based PVP-C with the same or the alternate template molecule is investigated in more detail and results are shown in Figure 4(b,c) using a four-cycle multi-indentation function. Reloading of the molecule that was not the original template alters the mechanical properties of the functional state. The results indicated that the slightly larger cotinine molecule could be inserted in the PVP-N system and an increase of hardness and reduced modulus in comparison to the as produced PVP-N state and nicotine reloaded PVP-*N*-N functional state was observed. This is reflected in the load-displacement curves in Figure 4(b). On the other hand, the reloading of the smaller nicotine molecule into the PVP-C system created a softer material, Figure 4(c), as the molecular pore is not completely filled and the hydrogen bonding to the polymer is altered. The result is that the PVP-C-N functional state has a lower hardness and a lower reduced modulus than that of the as produced PVP-C functional state or that of the nicotine reloaded PVP-*N*-N film. However, these values are still larger than those for the as produced nicotine imprinted PVP-N film.

The nanomechanical behavior of the polymer films is summarized graphically in Figure 5 and Table II with the average values of the depth dependent hardness and indentation modulus and their standard deviation. Hardness and indentation modulus values are fairly constant with indentation depth. At larger depth, a slight increase in both values is noticeable, which indicates contributions from the harder glass substrate. The hardness of the control PVP film has a value of 0.38 GPa with an indentation modulus of 11.7 GPa. MIP films with cotinine, PVP-C, are stiffer with a hardness value of 0.59 GPa and an indentation modulus of 14.7 GPa. Nicotine-imprinted films, PVP-N, are slightly stiffer than the control film with a hardness value of 0.43 GPa and a modulus of 11.6 GPa. Extraction of the template molecules leaves the molecular cavities present in the polymer matrix, but the space they once occupied is empty. Thus, the network character and, therefore, the mechanical properties change; see the load-displacement curves in Figure 4(a). For example, the hardness for MIP films with nicotine extracted yields a smaller value of 0.31 GPa for the hardness. Reloading nicotine into a nicotine-imprinted film from which the template has been removed or cotinine into an extracted cotinine-imprinted film results in a film with greater nanohardness than the original as produced film. The percentage increase in hardness is greater for the

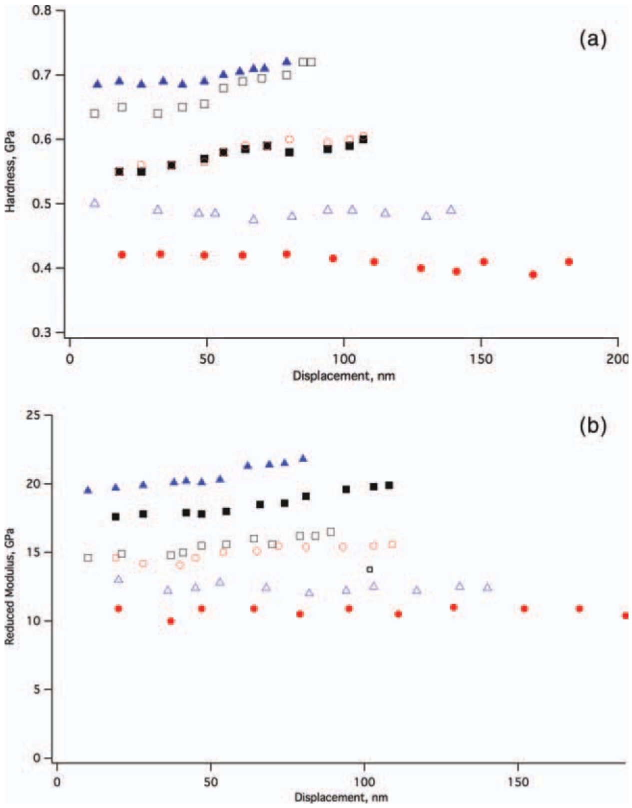

Figure 5 Depth-dependent hardness and reduced elastic modulus results for various functional states of the imprinted polymers. PVP-X indicates an "as produced" MIP N = nicotine and C = cotinine); PVP-X-Y indicates a MIP imprinted with X, which is subsequently removed and Y is inserted from solution. Legend: ●, PVP-N; ■, PVP-NN; ▲, PVP-NC and ○, PVP-C; □, PVP-CC; △, PVP-CN. [Color figure can be viewed in the online issue, which is available at wileyonlinelibrary.com.]

reinsertion of nicotine into a nicotine-targeted MIP than for cotinine into a cotinine-targeted MIP. In addition, cross reloading, that is nicotine in to an extracted cotinine-imprinted film or vice versa, measured hardness is greater than that of an as produced film for the reloading component. Loading, extraction and reloading of nicotine or cotinine in the MIP films are clearly measurable with the nanoindentation technique. Therefore, the different functional states can be distinguished by nanoindentation.

These results support the model of a strongly hydrogen-bonded network among the polymer chains via template molecular linkers. In the ideal case, a molecular cavity with a nicotine template molecule is formed with two hydrogen bonds that crosslink two PVP molecules; cotinine has three such potential hydrogen bonding sites. However, the imprinting process can be incomplete with fewer than the maximum number of hydrogen bonds established. Template molecules can bond to the polymer molecule at several points along the chain with efficiencies dependent upon the number and distribution of template molecules in the MIP film. From the nanomechanical investigations, it is suggested that hydrogen bonding of the template molecules between the PVP chains: (1) results in a cross-linking between the chains, (2) separates the PVP molecules (preventing an easy movement of the chains), and (3) reduces the adhesion energy between pure PVP molecules. This may result in both mechanically stiffer and softer MIP networks. We suggest two different molecular mechanisms for the polymer response during an applied external contact pressure. In pure PVP, the indentation tip can cause a deformation of the PVP molecules and a sliding motion between the chains. The molecular cavities and micropores change the mechanical properties in two directions compared to pure polymer films. Filled cavities (template loaded MIP) show an increase in hardness in comparison to pure PVP films. This implies that a stiffer molecular network is established. In MIP films, the chains are fixed by hydrogen bonds and the sliding motion is inhibited in general. The filled molecular cavities prevent strong elastic deformation. Empty cavities, after extraction of the template, result in a decrease in the hardness. This could be attributed to the empty MIP network more easily squeezed together (the empty cavities act as structural defects), resulting in a lower hardness in comparison to the pure polymer network. In MIP films, the PVP chains are fixed by the hydrogen bonds and the formed molecular cavities, but the deformation around the empty cavities is flexible (breathing cavities). Therefore, no gliding motion of the chains occurs. This means, the main effect for the change of the mechanical properties in different stages of MIP films originates from the formed molecular cavities. If they are filled with the template molecule the material is harder; if the cavities are empty, the compression of the cavities leads to a much softer material. The elastic compression of the empty cavities and pores acts in the same

TABLE II
Hardness and Elastic Modulus Values for Nicotine- and Cotinine-Imprinted PVPs

Template/Functional State[a]	H (GPa)	E (GPa)
PVP-N	0.41 ± 0.03	11.1 ± 1.89
PVP-N-N	0.58 ± 0.04	18.9 ± 2.9
PVP-N-C	0.7 ± 0.03	20.0 ± 2.1
PVP-C	0.59 ± 0.03	14.7 ± 1.2
PVP-C-C	0.69 ± 0.04	15.7 ± 1.2
PVP-C-N	0.48 ± 0.01	12.6 ± 0.6

[a] Functional state definition: PVP-X indicates an "as produced" MIP where N = nicotine and C = cotinine); PVP-X-Y indicates a MIP imprinted with X, which is subsequently removed and Y is inserted from solution.

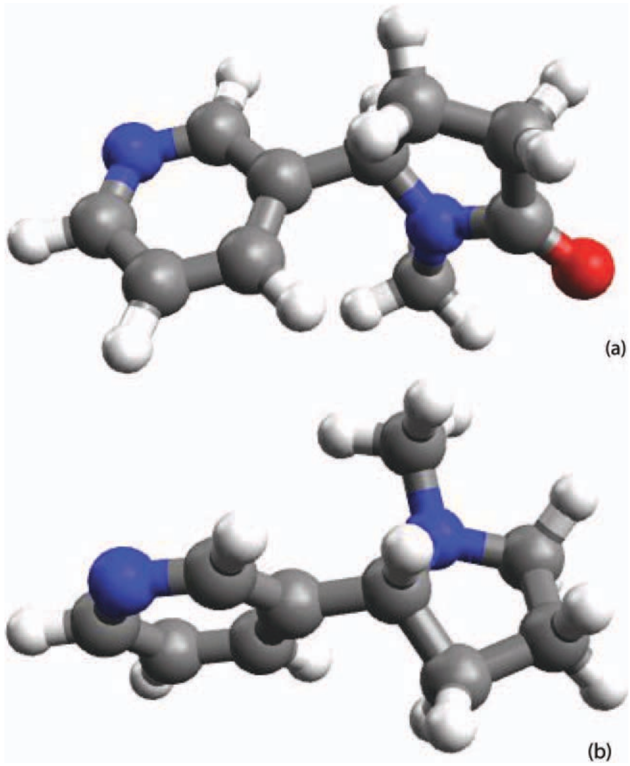

Figure 6 Optimized structures for the cotinine (a) and nicotine (b) imprint molecules. [Color figure can be viewed in the online issue, which is available at wileyonlinelibrary.com.]

direction as the mechanism of deformation and gliding of the PVP chains.

Computational study of hydrogen bonding

Reports in the literature indicate the usefulness of computational chemistry in selecting a polymer host for MIP development with a particular target molecule.[31] However, computational studies may also be useful in providing information to understand experimental MIP results, the task to which we have applied DFT here. The optimized structures of nicotine and cotinine were first obtained for reference and are shown in Figure 6 with the coordinates provided in Supporting Information Table I. These molecules differ only by the addition of a carboxyl group on the pyrrolidine ring of cotinine. The geometry of the planar pyridine ring, including bond lengths, in the two molecules is identical and they differ little in overall size, leading to some expectation that it would be possible to cross-load MIPs templated for one or the other of these related molecules. The presence of the oxygen atom in cotinine results in bond shortening in the pyrrolidine ring, as well as a further distortion from planarity relative to the nicotine pyrrolidine ring. The pyrrolidine nitrogen becomes more sp^2-like rather than the pyramidal angle observed in the nicotine molecule. As a final reference point, the 4-vinylphenol (4VP) dimer structure was optimized and was found to have a hydrogen bond length of 1.876 Å and a hydrogen bond energy of 0.34 eV. The geometric parameters of the monomeric 4-vinylphenol molecule are unchanged in the dimer.

Nicotine has two potential hydrogen binding sites and cotinine has three such sites. The optimized structures for the interaction of nicotine with two monomers and cotinine with three are shown in Figure 7. In both clusters, the optimized 4-vinylphenol geometry is identical to that of the unbonded

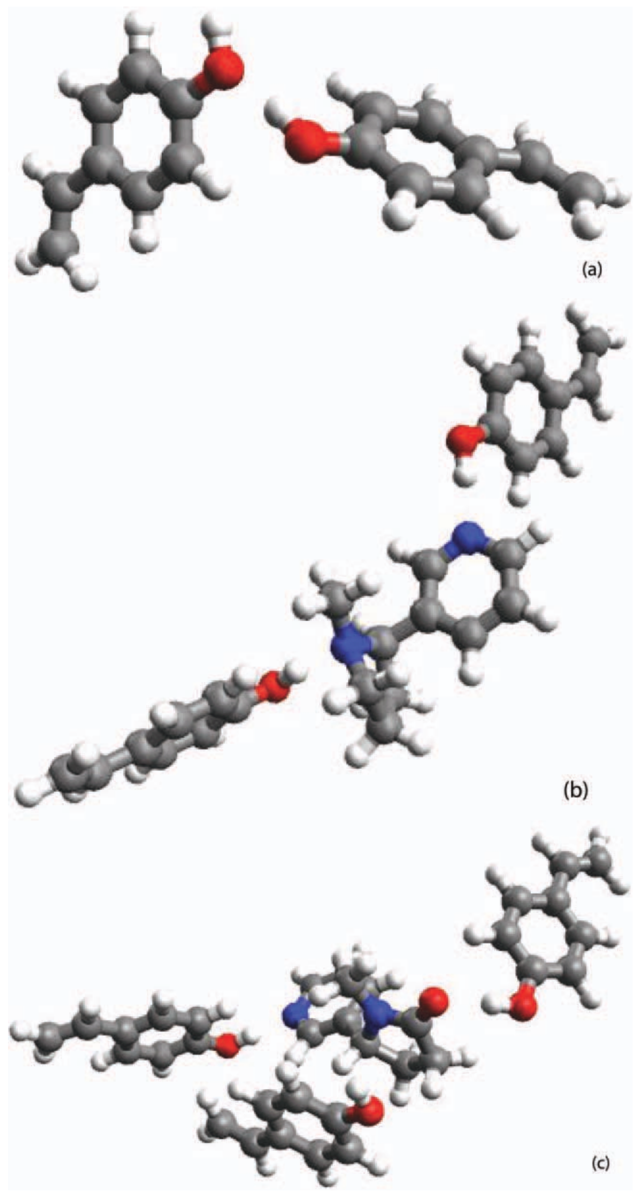

Figure 7 Optimized hydrogen bonded structures for (a) a 4VP dimer, (b) a nicotine plus two 4VP molecular cluster, and (c) a cotinine plus three 4VP molecular cluster. [Color figure can be viewed in the online issue, which is available at wileyonlinelibrary.com.]

molecule and the pyridine ring bond lengths are unaffected by the hydrogen bond. The hydrogen bond from 4VP to the pyridine nitrogen in nicotine has a length of 1.822 Å, whereas that to the pyrrolidine nitrogen is 1.788 Å. The C—N bond lengths in this ring both increase. The total hydrogen bonding energy is 0.84 eV. In cotinine, only two hydrogen bonds form. The bond to the pyridine nitrogen has a length of 1.820 Å and that to the carboxyl-oxygen is 1.784 Å with a total hydrogen bonding energy of 1.00 eV. Attempts to add a third hydrogen bond at the pyrrolidine nitrogen site fail, as the additional PVP molecule is repulsed from the ring. The C—N bond lengths in the pyrrolidine ring both decrease upon hydrogen bonding. Finally, we note that attempts to obtain a π-π complex between cotinine and 4VP indicate that the ring interactions are repulsive. Clearly, the DFT calculations indicate that cotinine will complex to the PVP host matrix with a greater binding energy than the nicotine template, forming a stiffer network, and the experimental results reflect the results of those calculations.

General discussion

The mechanical properties of the nicotine and cotinine templated PVP MIPs differ from the amino acid samples investigated earlier,[14] as in this study, the matrix with the reinserted template molecules has a greater hardness compared to the "as-produced" MIP polymer state. The hardness and the reduced modulus increase dramatically from 0.41 GPa and 11.1 GPa for the "as-produced" state, PVP-N, to 0.58 GPa and 18.9 GPa for the reloaded state, PVP-*N*-N. This represents a hardness and modulus increase of 41 and 70%, respectively. The same responses are observed for the PVP-C material system, although the effect on a percentage basis is less pronounced. Here, the hardness and the reduced modulus increase from 0.59 GPa and 14.7 GPa for the "as-produced" state, PVP-C, to 0.69 GPa and 15.7 GPa for the reloaded state, PVP-C-C. The hardness increases by 17% and the modulus by 7%. The DFT calculations predicted that the cotinine molecule would hydrogen bond more strongly with the polymer PVP matrix than the nicotine molecule. Therefore, the PVP-C MIP would be more stable than the PVP-N functional state. This is reflected experimentally in a larger hardness and reduced modulus for the PVP-C "as-produced" system. Reloading of the complementary molecule results in mechanical properties approaching those of the as-produced MIP of the reinserted material; insertion of the cotinine molecule into the PVP-N template removed MIP results in an increase of hardness and reduced modulus by 75 and 80%, respectively. Differing geometric parameters and bonding generate a strong increase of the mechanical parameters. On the other hand, the reloading of the nicotine molecule into the PVP-C template removed MIP system creates a softer material, as the hydrogen bonding of this molecule to the polymer is weaker than that of the original cotinine template; the PVP-C-N functional state presents a 19% lower hardness and a 14% lower modulus than the "as produced" PVP-C state. These values are similar to those of the "as-produced" PVP-N system. The trend is clear; for both systems, we have found that the reinsertion of the molecule for which the MIP has been templated makes the material stiffer than in the "as-produced" state, even though the extent of reinserted is 50% of the original film content. This behavior may be attributed to the fact that reintroduction of the template occurs primarily in the upper portion of the film and nanoindentation is sampling exactly this region. The increase in nanohardness with reinsertion of the analyte molecule is unique among the MIPs we have studied. In other studies, we have found that reinsertion of the analyte returns the nanomechanical properties to approximately, but slightly less than, those of the originally produced MIP.[14] The observation here, in a MIP that is considerably less porous than those for carbohydrates or amino acids, may be attributed to shrinkage of a film from which the template has been extracted during the aging process. PVP is known to provide gas-tight coatings in the case of polymer-coated foam shells.[32] In those same studies, the PVP coating was found to cause a densification of the foam core as the coating underwent shrinkage. If the bulk of the MIP film experienced the same shrinkage, in the extracted state, reinsertion of the template molecule (or the alternative analyte) would result in hydrogen bonding but not necessarily entirely within the molecular cavities. The hydrogen bond strengths would not necessarily differ, but the overall nanomechanical properties would be altered by these additional, nonspecific hydrogen bonds. As observed experimentally the control films exposed to the same treatment as the MIPs would not experience this effect, as the macropores and the molecular cavities were not present in the NIPs.

CONCLUSIONS

We have measured the nanomechanical properties of nicotine- and cotinine-imprinted poly(4-vinylphenol) films using depth sensing nanoindentation. These measurements have shown that:

- changes in the nanomechanical properties are correlated to the functional state of the imprinted polymer, allowing identification of the films in their "as produced" state, "template removed" state or "reloaded" state;

- the nanomechanical properties are capable of identifying which of the two template molecules, nicotine or cotinine, are inserted into a film when the templates are cross-introduced into emptied MIPs;
- the nanomechanical properties reflect the hydrogen bonding characteristics of the template molecules as determined through DFT calculations;
- reinsertion of a template molecule into a "template removed" film increases the nanohardness over the values recorded for the "as produced" film as a result of the physical properties of the polymer.

These results indicate that nanohardness measurements may be used as a reporting tool in the development of a new generation of sensors.

J. J. B. acknowledges the support of the Flight Attendants Medical Research Institute through the Richmond Center for Excellence of the American Academy of Pediatrics.

References

1. Marty, J. D.; Mauzac, M. Adv Polym Sci 2005, 172, 1.
2. Dufaud, V.; Bonneviot, L. In Nanomaterials and Nanochemistry; Brechignac, C., Houdy, P., Lahmani, M., Eds.; Springer: Berlin, 2008; p 597.
3. Kempe, H.; Kempe, M. In the Power of Functional Resins in Organic Synthesis; Tulia-Puche, J., Fibericio, F., Eds.; Wiley: Berlin, 2008.
4. Poma, A.; Turner, A. P. F.; Piletsky, S. A. Trends Biotechnol 2010, 28, 629.
5. BelBruno, J. J. Micro Nanosyst 2009, 1, 163.
6. Yanga, K.; Maa, J.; HZhoub, H.; Lia, B.; Yua, B.; Zhaoa, C. Desalination 2009, 245, 232.
7. Faizala, C. K. M.; Kikuchic, Y.; Kobayashi, T. J Membr Sci 2009, 334, 110.
8. Dima, S. O.; Sabru, A.; Dobre, T.; Bradu, C.; Antohe, N.; Radu, A.; Nicolescui, T.; Lungu, A. Mat Plastice 2009, 46, 372.
9. Chen, R. R; Qin, L.; Jia, M.; He, X. W.; Li, Y. J Membr Sci 2010, 363, 212.
10. Shneskoff, N.; Crabb, K.; BelBruno, J. J. J Appl Polym Sci 2002, 86, 3611.
11. Richter, A.; Gibson, U. J.; Nowicki, M.; BelBruno, J. J. J Appl Polym Sci 2006, 101, 2919.
12. Campbell, S. E.; Collins, M.; Lei, X.; BelBruno, J. J Surf Interface Anal 2009, 41, 347.
13. Sambe, H.; Hoshina, K.; Moaddel, R.; Wainer, I. W.; Haginaka, J. J Chromatogr A 2006, 1134, 88.
14. BelBruno, J. J.; Richter, A.; Campbell, S. E.; Gibson, U. J. Polymer 2007, 48, 1679.
15. Richter, A.; Gruner, M.; BelBruno, J. J.; Gibson, U. J.; Nowicki, M. Colloids Surf A 2006, 284/285, 401.
16. Fischer-Cripps, A. C. Nanoindentation; Springer: New York, 2002.
17. Olivier, W. C.; Pharr, G. M. J Mater Res 1992, 7, 1562.
18. Wolf, B.; Richter, A. New J Phys 2003, 5, 15.
19. IWard, I. M.; Hadley, D. W. An Introduction to the Mechanical Properties of Solid Polymers; John Wiley: Chichester, 1993.
20. Nowicki, M.; Richter, A.; Wolf, B.; Kaczmarek, H. Polymer 2003, 44, 6599.
21. Du, B.; Liu, J.; Zhang, Q.; He, T. Polymer 2000, 42, 5901.
22. Tsui, O. K.; Wang, X. P.; Ho, J. Y. L.; Nag, T. K.; Xiao, X. Macromolecules 2000, 33, 4198.
23. Richter, A.; Smith, R. Encyclopedia Nanosci Nanotechnol 2011, 17, 375.
24. Bronside, D. E.; Macosko, C. W.; Scriven, L. E. J Imaging Technol 1987, 13, 122.
25. Hysitron Inc. Hysitron User Handbook: Feedback Control Manual. Hysitron, Inc: Minneapolis, USA.
26. Richter, A.; Smith, R.; Dubrovinskaia, N.; Mcgee, E. High Pressure Res 2006, 26, 99.
27. Valiev, M.; Bylaska, E. J.; Govind, N.; Kowalski, K.; Straatsma, T. P.; van Dam, H. J. J.; Wang, D.; Nieplocha, J.; Apra, E.; Windus, T. L.; de Jong, W. A. Comput Phys Commun 2010, 181, 1477.
28. Adamo, C.; Barone, V. J Chem Phys 1998, 110, 6158.
29. Hariharan, P. C.; Pople, J. A. Theor Chim Acta 1973, 28, 213.
30. Avogadro, GNU Project. Available at: http://avogadro.openmolecules.net.
31. Breton, F.; Rouillon, R.; Pilestska, E. V.; Karim, K.; Guerreiro, A.; Chianella, I.; Piletsky, S. A. Biosens Bioelectron 2007, 22, 1948.
32. Nikroo, A.; Czechowicz, D.; Paguio, R.; Greenwood, A. L.; Takagi, M. Presented at the15th Target Fabricartion Specialists Meeting; Gleneden Beach, Oregon, June 1–5, 2003. General Atomics Report. Available at: https://fusion.gat.com/pubs-ext/TFSM03/A24451.pdf.